Supporting Information

Single-Particle Assay of Poly(ADP-ribose) Polymerase-1 Activity with Dark-Field Optical Microscopy

Duoduo Zhang, Kan Wang, Wei Wei*, Songqin Liu

Jiangsu Engineering Laboratory of Smart Carbon-Rich Materials and Device, Jiangsu Province Hi-Tech Key Laboratory for Bio-medical Research, School of Chemistry and Chemical Engineering, Southeast University, Nanjing, 211189, China

*Corresponding author. Tel.: 86-25-52090613; Fax: 86-25-52090618.

E-mail address: weiw@seu.edu.cn (W. Wei)

15 **Table of contents**

35

36

Materials. All oligonucleotides listed in Table S1 were sythesized by Shanghai Sangon biotechnology (Shanghai, China). Bis(p-sulfonatophenyl)phenylphosphine (BSPP) and nicotinamide adenine dinucleotide (NAD^+) were purchased from Sigma-Aldrich (Shanghai, China). (3-aminopropyl)-triethoxysilane (APTES) was purchased from Macklin Biochemical (Shanghai, China). Hexadecyltrimethylammonium bromide (CTAB) was obtained from J&K Scientific Ltd. (Beijing, China). Trisodium citrate, chloroauric acid tetrahydrate ($HAuCl_4 \cdot 4H_2O$) and polyvinylpyrrolidone (PVP) were purchased from Sinopharm Chemical Reagent (Shanghai, China). Gold chloride trihydrate ($HAuCl_4 \cdot 3H_2O$) was obtained from Energy Chemical (Shanghai, China). Human PARP-1 was obtained from Trevigen (Wuhan, China). Dulbecco's Modified Eagle Medium (DMEM) medium, RPMI-1640 medium, fetal bovine serum (FBS) and 3-(4,5-dimethylthiazol-2-yl)-2-diphenyltetrazolium bromide (MTT) were all from KeyGen Biotech (Nanjing, China). The formation of PAR catalyzed by PARP-1 was operated in the reaction buffer solution (R-buffer) composed of 50 mM Tris-HCl, 2 mM $MgCl_2$, 50 μM $Zn(OAc)_2$ and 50 mM KCl (pH 7.4). Ultrapure water (18.2 MΩ·cm at 25 ^oC, Thermo Scientific, USA) was used in the whole assay. All other reagents were of analytical grade and needed no further treatment.

Apparatus. Transmission electron microscopy (TEM) images were carried out with a Tecnai G2 20 (FEI, Czech Republic). Scanning electron microscopy (SEM) images were obtained with a JSM-7001F SEM (JEOL, Japan). The ultraviolet-visible (UV-vis) absorption spectra were recorded with UV-visible spectrometer (Shimadzu UV-2450,

Kyoto, Japan). Zeta potentials of each sample were all measured by NanoBrook Omni Zeta potential analyzer (Brookheaven, USA) at 25 °C and measurements were performed at least three times after diluted by deionized (DI) water. An inverted optical microscopy (Eclipse Ti-E, Nikon, Japan) equipped with a dark field condenser ($0.8 < NA < 0.95$) and a 60X objective lens (NA = 0.7) was used for dark-field spectroscopic experiments. White light source (100 W halogen lamp) through condenser was focused onto the sample and excited the nanoprobes to generate plasmon resonance scattering light. After collected by a 60X objective and captured by a true color digital camera (Nikon digital sight DS-Ri1, Japan), the scattering light was split by a monochromator (Acton, P-2300, Princeton Instruments, USA) equipped with a grating (grating density: 50 $g \cdot mm^{-1}$; blazed wavelength: 600 nm). Then a spectrometer charge-coupled device (CCD) (PyLoN, Princeton Instruments, USA) was utilized to record the scattering spectra. In order to avoid interference and ensure accuracy, all scattering spectra of the nanoprobes were corrected by subtracting the background spectrum generated by the instrument itself.

Synthesis of Gold Nanoparticles. The synthesis process of AuNPs with size of 13 nm (Au_{13}) was according to trisodium citrate-based classic reduction method. In brief, an aqueous solution of $HAuCl_4 \cdot 4H_2O$ (1 mM, 50 mL) was poured into the round-bottom flask and brought to a vigorous boil while stirring. Once the gold solution started to reflux vigorously, trisodium citrate solution (38.8 mM, 5 mL) was added rapidly into $HAuCl_4$ solution. The color of the mixture solution changed from yellow to clear, to black, to purple and finally to wine red throughout the whole

81 reaction process. Fifteen minutes later, the heating source was removed and the
82 obtained solution was allowed to cool to room temperature (RT). Finally, the colloidal
83 solution was stored in a brown glass bottle at 4 °C for further use.

84 The seed-growth method was used for preparation of Au_{50}. Briefly, 1 mL of the
85 above prepared Au_{13} (used as seed), 25 mL of DI water, 360 μL of 0.2 M
86 $NH_2OH{\cdot}HCl$ solution and 300 μL of 1 % w/v PVP (44000-54000 MW) were mixed in
87 a 50 mL round-bottom flask in sequence. Then 8 mL of 0.1 wt % $HAuCl_4$ was
88 injected dropwise into the mixture within 30 min under violent stirring at RT. The
89 reaction was stopped after another 30 min. Finally, the obtained Au_{50} was stored in a
90 brown glass bottle at 4 °C for further use. The concentration of the Au_{50} solution was
91 estimated to be 0.1 nM, which was calculated by the Lambert-Beer law with the
92 extinction coefficient of $1.5 \times 10^{10}{\cdot}M^{-1}{\cdot}cm^{-1}$.[1]

93 **Extraction of Cytoplasm and Nucleus of Cells.** The extractive cytoplasm and
94 nucleus of two kinds of cancer cells (A2780 and MCF-7) and normal cells (IOSE80)
95 were obtained according to the previously reported method.[7] Firstly, A2780 cells were
96 washed by 1 × PBS (pH 7.4) one time or treated by ethylenediaminetetraacetic acid
97 (EDTA). Then the obtained cells were centrifuged with discarding supernatant.
98 Subsequently the cytoplasmic protein and nuclear extraction reagent were added
99 separately followed by vigorous shaking. The resulting mixture was centrifuged at
100 12000 rpm at 4 °C for 5 min. Finally, the obtained supernatants of cytoplasm and
101 nuclei were stored respectively in precooling centrifuge tubes at -80 °C for further use.
102 Cytoplasm and nucleus protein from MCF-7 and IOSE80 were also extracted on the

103 basis of our previous study.

104 **Preparation of Au_{50}-dsDNA-aptamer.** Firstly, excess BSPP was added to 1 mL of
105 Au_{50} solution. And the mixture was incubated at RT overnight under stirring, which
106 replaced the citrate ligands on the surface of Au_{50} with BSPP ligands and stabilized
107 AuNPs at high ionic strength in the process of DNA modification. Then the mixture
108 was centrifuged at 8000 rpm for 15 min to collect the precipitation which was
109 redispersed in 1 mL of DI water. 50 μL of 10 mM BSPP was then added to the
110 solution and shaked uniformly to obtain Au_{50}-BSPP. Secondly, the resulting
111 BSPP-protected Au_{50} was mixed with 30 μL of 1 μM specific-DNA (s-DNA) and 30
112 μL of 1 μM AS1411 aptamer, followed by gently rocking at RT for 12 h. For
113 enhancing the salt resistance of Au_{50}, 1 M NaCl was introduced every 3 h until the
114 final concentration up to 150 mM. After that, 18 μL of 10 μM thiol-polyethylene
115 glycol 800 (PEG-800) was added to the above Au_{50} solution with incubation for 1 h to
116 block nonspecific binding sites of AuNPs. Thirdly, 30 μL of 1 μM complementary
117 DNA (c-DNA) was added with gentle vortexes for 2 h to realize the modification of
118 activated dsDNA on the Au_{50} surface. Finally, the Au_{50}-dsDNA-aptamer was collected
119 by centrifugation at 8000 rpm for 15 min.

120 **Preparation of Au_8-aptamer.** Firstly, 30 μL of 1 μM AS1411 aptamer was added to
121 1 mL of Au_8 solution, followed by gently rocking at RT for 12 h. Then, the
122 Au_8-aptamer was collected by centrifugation at 13000 rpm for 15 min.

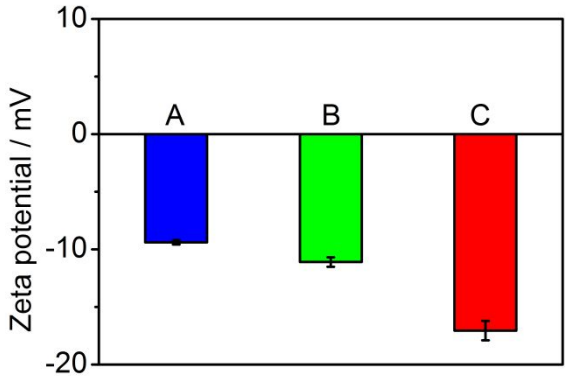

Figure S1. Zeta potentials of individual Au_{50} (A), Au_{50}-dsDNA (B) and Au_{50}-dsDNA@PAR (C). 5.0 mU PARP-1 was used for forming Au_{50}-dsDNA@PAR. The error bars represent standard deviations of three repetitive measurements.

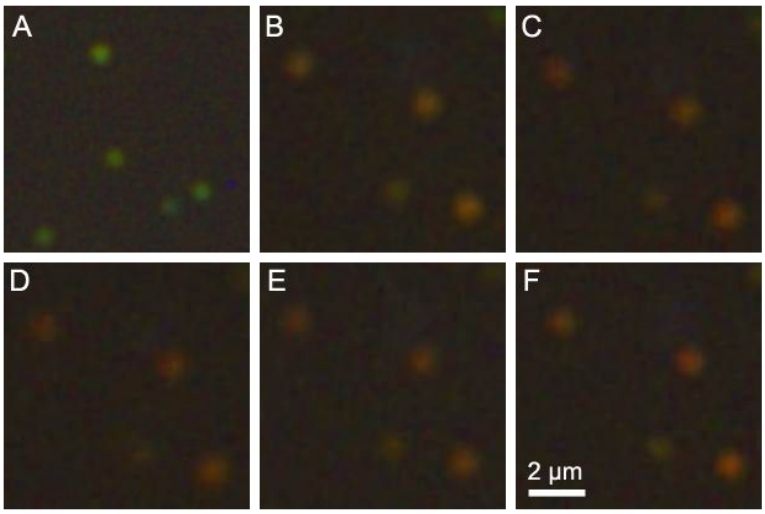

Figure S2. (A) Dark-field images of Au_{50}-dsDNA without Au_8. Real-time dark-field images of Au_{50}-dsDNA@PAR incubated with Au_8 for different times: (B) 0, (C) 5, (D) 10, (E) 20 and (F) 30 min. 5.0 mU PARP-1 was used for the optimization.

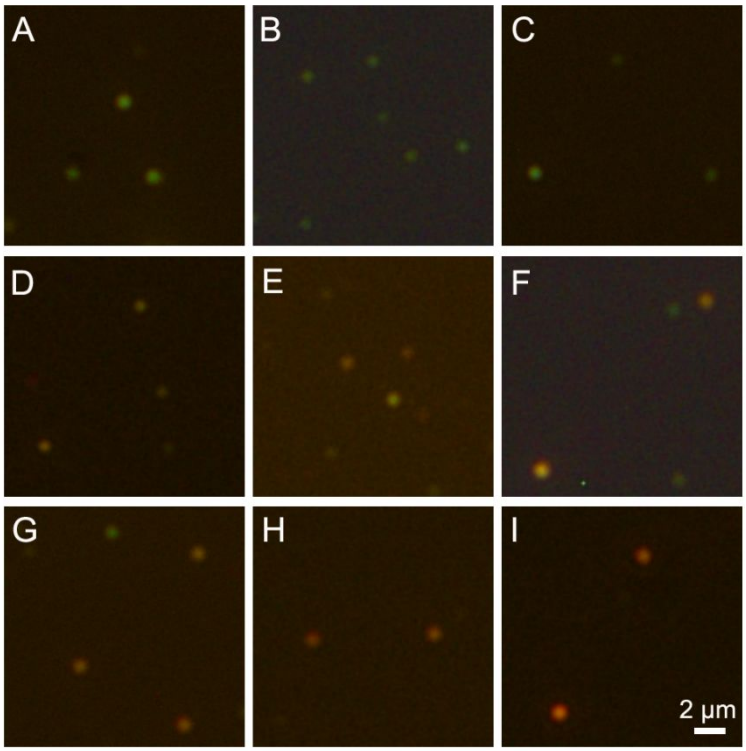

Figure S3. Dark-field images of control assay without PARP-1: (A) Au_{50}, (B) Au_{50}-dsDNA, (C) Au_{50}-dsDNA + NAD^+, then incubated with Au_8. Representative dark-field images of Au_{50}-dsDNA incubated with NAD^+, Au_8 and PARP-1 with different concentrations: (D) 0.2, (E) 0.3, (F) 1.0, (G) 2.0, (H) 5.0 and (I) 10 mU.

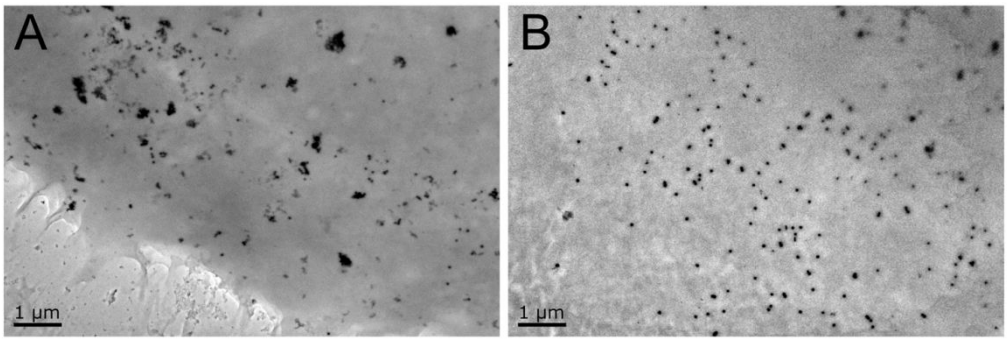

Figure S4. TEM images of MCF-7 cells (A) and IOSE80 cells (B) incubated with 10 pM Au_{50}-dsDNA-aptamer for 5 h and followed incubation with Au_8-aptamer for 1 h at low magnification.

Table S1. Sequences of oligonucleotides employed in this work.

Name	Sequence and modifications (from 5' - 3')
Specific DNA	HS-$(CH_2)_6$-CCCGTGCGTGCGCGAGTGAGTTG
Complementary DNA	CAACTCACTCGCGCACGCACGGG
AS1411 aptamer	HS-$(CH_2)_6$-GGTGGTGGTGGTTGTGGTGGTGGTGG

Table S2. Comparison of analytical performances of various methods for determination of PARP-1.

Method	System	Detection range	LOD	Reference
ELISA	PARP-1 antibody	Semiquantitative	-	2
PAGE	Clickable NAD^+	Qualitative	-	3
Fluorescence	NAD^+ analogue	Qualitative	-	4
Fluorescence	MnO_2 quenched PFP	0.03-1.5 U	0.004 U	5
Fluorescence	TOTO-1	0.02-1.5 U	0.02 U	6
UV-Vis	AuNRs aggregation	0.05-1 U	0.006 U	7
Photoelectrochemistry	PFP	0.01-2 U	0.007 U	8
Nanochannel	Diffusion flux	0.05-1.5 U	0.006 U	9
Single nanoparticle scattering spectrum	AuNPs	0.2-10 mU	-	This work

Table S3. Detection of PARP-1 in cancer cells by the clinical ELISA method.

Cancer cells	Found (U) in Nuclei	Found (U) in Cytoplasm
A2780	0.3091	0.1313
MCF-7	0.2336	0.1358

REFERENCES

(1) Zhang, X.; Gouriye, T.; Göeken, K.; Servos, M. R.; Gill, R.; Liu, J. W. Toward Fast and Quantitative Modification of Large Gold Nanoparticles by Thiolated DNA: Scaling of Nanoscale Forces, Kinetics, and the Need for Thiol Reduction. *J. Phys. Chem. C* **2013**, *117*, 15677-15684.

(2) Decker, P.; Miranda, E. A.; Murcia, G. De; Muller, S. An Improved Nonisotopic Test to Screen a Large Series of New Inhibitor Molecules of Poly(ADP-ribose) Polymerase Activity for Therapeutic Applications. *Clin. Cancer Res.* **1999**, *5*, 1169-1172.

(3) Wang, Y.; Rösner, D.; Grzywa, M.; Marx, A. Chain-Terminating and Clickable NAD^+ Analogues for Labeling the Target Proteins of ADP-Ribosyltransferases. *Angew. Chem. Int. Edit.* **2014**, *53*, 8159-8162.

(4) Buntz, A.; Wallrodt, S.; Gwosch, E.; Schmalz, M.; Beneke, S.; Ferrando-May, E.; Marx, A.; Zumbusch, A. Real-Time Cellular Imaging of Protein Poly(ADP-ribos)ylation. *Angew. Chem. Int. Edit.* **2016**, *55*, 11256-11260.

(5) Wu, S. S.; Chen, C. H.; Yang, H. T.; Wei, W.; Wei, M.; Zhang, Y. J.; Liu, S. Q. A sensitive fluorescence "turn-off-on" biosensor for poly(ADP-ribose) polymerase-1 detection based on cationic conjugated polymer-MnO_2 nanosheets. *Sens. Actuators, B* **2018**, *273*, 1047-1053.

(6) Yang, H. T.; Fu, F. J.; Li, W.; Wei, W.; Zhang, Y. J.; Liu, S. Q. Telomerase and poly(ADP-ribose) polymerase-1 activity sensing based on the high fluorescence selectivity and sensitivity of TOTO-1 towards G bases in single-stranded DNA and

poly(ADPribose). *Chem. Sci.* **2019**, *10*, 3706-3714.

(7) Wu, S. S.; Wei, M.; Yang, H. T.; Fan, J. H.; Wei, W.; Zhang, Y. J.; Liu, S. Q. Counterions-mediated gold nanorods-based sensor for label-free detection of poly(ADP-ribose) polymerase-1 activity and its inhibitor. *Sens. Actuators B Chem.* **2018**, *259*, 565-572.

(8) Wang, C. C.; Li, Y.; Xu, E. S.; Zhou, Q.; Chen, J.; Wei, W.; Liu, Y.; Liu, S. Q. A label-free PFP-based photoelectrochemical biosensor for highly sensitive detection of PARP-1 activity. *Biosens. Bioelectron.* **2019**, *138*, 1-6.

(9) Liu, Y.; Fan, J. H.; Yang, H. T.; Xu, E. S.; Wei, W.; Zhang, Y. J.; Liu, S. Q. Detection of PARP-1 Activity based on Hyperbranched-Poly (ADP-ribose) Polymers Responsive Current in Artificial Nanochannels. *Biosens. Bioelectron.* **2018**, *113*, 136-141.